eNeuro

Research Article: Open Source Tools and Methods | Novel Tools and Methods

Neuron replating – a powerful and versatile approach to study early aspects of neuron differentiation

https://doi.org/10.1523/ENEURO.0536-20.2021

Cite as: eNeuro 2021; 10.1523/ENEURO.0536-20.2021

Received: 27 November 2020
Revised: 12 April 2021
Accepted: 20 April 2021

This Early Release article has been peer-reviewed and accepted, but has not been through the composition and copyediting processes. The final version may differ slightly in style or formatting and will contain links to any extended data.

Alerts: Sign up at www.eneuro.org/alerts to receive customized email alerts when the fully formatted version of this article is published.

Copyright © 2021 Schneider et al.
This is an open-access article distributed under the terms of the Creative Commons Attribution 4.0 International license, which permits unrestricted use, distribution and reproduction in any medium provided that the original work is properly attributed.

eNeuro Accepted Manuscript

eNeuro Accepted Manuscript

1 **Title page**

2 **Manuscript title**

3 Neuron replating – a powerful and versatile approach to study early aspects of
4 neuron differentiation

5 **Abbreviated title**

6 Neuron replating protocol

7 **Authors**

8 Felix Schneider[1,2,3,], Thuy-An Duong[1], Marco B. Rust[1,2,3,4]

9 [1]Molecular Neurobiology Group, Institute of Physiological Chemistry, University of Marburg, 35032
10 Marburg, Germany; [2]Center for Mind, Brain and Behavior (CMBB), University of Marburg and Justus-
11 Liebig-University Giessen, 35032 Marburg, Germany; [3]DFG Research Training Group, Membrane
12 Plasticity in Tissue Development and Remodeling, GRK 2213, Philipps-University of Marburg, 35032
13 Marburg, Germany

14 **[4]Correspondent author**

15 Marco B. Rust

16 Institute of Physiological Chemistry, University of Marburg

17 35032 Marburg, Germany

18 Phone: +49-6421-2865020, E-Mail: rust@uni-marburg.de

19 **Number of figures**

20 6

21 **Number of tables**

22 none

23 **Number of multimedia**

24 4

25 **Number of words for abstract**

26 252

27 **Number of words for significance statement**

28 124

Number of words for introduction

372

Number of words for discussion

1,150

Acknowledgements

We thank Mrs. Renate Gondrum for excellent technical support, Dr. Robert Grosse (University of Freiburg, Germany) for GFP-actin and LifeAct-GFP constructs, Dr. David Solecki (St. Jude Children's Research Hospital Memphis, USA) for mCherry-Cre constructs and Dr. Walter Witke (University of Bonn, Germany) for ADF$^{-/-}$/Cfl1$^{flx/flx}$ mice.

Funding sources

This work was supported by a research grant from the Deutsche Forschungsgemeinschaft (DFG) to MBR (RU 1232/7-1). FS was funded by the DFG Research Training Group ‘Membrane Plasticity in Tissue Development and Remodeling’ (GRK 2213).

Author Contributions

Experiments were performed and analyzed by FS and TAD, experiments were designed by FS and MBR, manuscript was written by MBR and FS.

Conflict of Interest

Authors report no conflict of interest

eNeuro Accepted Manuscript

eNeuro Accepted Manuscript

51 ## Abstract

52 Neuron differentiation includes formation and outgrowth of neurites that differentiate
53 into axons or dendrites. Directed neurite outgrowth is controlled by growth cones that
54 protrude and retract actin-rich structures to sense environmental cues. These cues
55 control local actin filament dynamics, steer growth cones towards attractants and
56 away from repellents and navigate neurites through the developing brain. Rodent
57 hippocampal neurons are widely used to study the mechanisms underlying neuron
58 differentiation. Genetic manipulation of isolated neurons including gene inactivation
59 or reporter gene expression can be achieved by classical transfections methods, but
60 these methods are restricted to neurons cultured for several days, after neurite
61 formation or outgrowth. Instead, electroporation allows gene manipulation prior to
62 seeding. However, reporter gene expression usually takes up to 24 hours and time
63 course of gene inactivation depends on the half live of the targeted mRNA and gene
64 product. Hence, these methods do not allow to study early aspects of neuron
65 differentiation. In the present study, we provide a detailed protocol in which we
66 combined electroporation-based gene manipulation of mouse hippocampal neurons
67 prior to initial seeding with a replating step after two days *in vitro* that resets neurons
68 into an undifferentiated stage. By categorizing neurons according to their
69 differentiation stage, thorough morphometric analyses, live imaging of actin
70 dynamics in growth cones as well as guidance cue-mediated growth cone
71 morphological changes, we demonstrate that differentiation and function of replated
72 neurons did not differ from non-replated neurons. In summary, we provide a protocol
73 that allows to thoroughly characterize differentiation of mouse primary hippocampal
74 neurons.

75

76 **Significance statement**

77 Unraveling the molecular mechanisms that control neuron differentiation requires
78 reporter gene expression or gene inactivation. In mouse primary hippocampal
79 neurons, a widely used cellular system to study neuron differentiation, classical
80 transfection methods are restricted to later stages of differentiation. Instead,
81 electroporation allows genetic manipulation prior to seeding. However, time course
82 of reporter gene expression or gene inactivation frequently hinders a full
83 characterization of neuron differentiation, specifically of early stages. To circumvent
84 this limitation, we combined electroporation-based genetic manipulation prior to initial
85 seeding with a replating step after two days *in vitro*, which reset neurons into an
86 undifferentiated stage. We show that replated neurons differentiated similar to non-
87 replated neurons. We provide a detailed protocol that allows to comprehensively
88 characterize the molecular mechanisms underlying neuron differentiation.

89

eNeuro Accepted Manuscript

eNeuro Accepted Manuscript

90 ## Introduction

91 During differentiation, neurons undergo striking morphological changes from spheres
92 to polar cells possessing an axon and a highly branched dendritic compartment (da
93 Silva et al., 2002; Dotti et al., 1988). Essential steps during early neuron
94 differentiation include the formation and outgrowth of neurites, which later
95 differentiate into axons or dendrites. Directed neurite outgrowth depends on growth
96 cones, structures at neurite tips enriched in actin filaments (F-actin) that steer
97 neurites towards attractants and away from repellent cues and, hence, navigate
98 neurites through the developing brain (Gomez et al., 2014). Cultured hippocampal
99 neurons isolated from mice or rats are widely used cellular systems to study neuron
100 differentiation as they readily polarize on a two-dimensional substrate at very low
101 densities (da Silva et al., 2002; Dotti et al., 1988). Genetic manipulation including
102 gene silencing, gene deletion or reporter gene expression provide powerful
103 approaches to study virtually all biological processes in cellular systems, including
104 neuron differentiation. Electroporation-based nucleofection as well as classical
105 transfection procedures such as liposome-based transfection or calcium phosphate
106 precipitation are the most commonly applied methods for gene transfer into cultured
107 hippocampal neurons as they are far less labor-intensive when compared to virus
108 infection (Dudek et al., 2001; Ohki et al., 2001; Sun et al., 2013; Viesselmann et al.,
109 2011; Zeitelhofer et al., 2009). Unfortunately, efficiency of classical transfection
110 procedures is rather low and these approaches are convenient only for hippocampal
111 neurons cultured for several days, e.g. at around six days *in vitro* (DIV6) or later.
112 Instead, nucleofection allows genetic manipulation of hippocampal neurons prior to
113 seeding. However, expression of reporter genes usually takes up to 24 hours and,
114 more importantly, time course and efficiency of gene silencing or gene deletion
115 depends on the half live of the targeted mRNA and gene product. Consequently,
116 nucleofection of hippocampal neurons does not allow a thorough analysis of neuron
117 differentiation, specifically not of early processes during neuron differentiation. Thus,
118 experimental approaches are needed to circumvent these limitations. We here report
119 a protocol to reset primary hippocampal neurons from embryonic mice at DIV2 into
120 an undifferentiated stage. Prior to initial seeding, these neurons can be manipulated
121 genetically by means of nucleofection. We show that a combination of nucleofection
122 and replating allows to study early aspects of neuron differentiation.

eNeuro Accepted Manuscript

124 ## Material and Methods

125 ### Mice

126 Generation of ADF$^{-/-}$/Cfl1$^{flx/flx}$ mice has been reported before (Bellenchi et al., 2007;
127 Wolf et al., 2015; Zimmermann et al., 2015). Mice were housed with food and water
128 available *ad libitum* on 12-hour dark-light cycles. Treatment of mice was in
129 accordance with the German law for conducting animal experiments and followed
130 the guidelines for the care and use of laboratory animals of the U.S. National
131 Institutes of Health. Sacrification of mice has been approved by internal animal
132 welfare authorities (references: AK-5-2014, AK-6-2014, AK-12-2020). Genetic
133 inactivation of Cfl1 in neurons from ADF$^{-/-}$/Cfl1$^{flx/flx}$ mice was achieved by
134 nucleofection of catalytic active mCherry-Cre. ADF$^{-/-}$/Cfl1$^{flx/flx}$ neurons expressing a
135 mutant, catalytic inactive mCherry-Cre served as controls. Both constructs have
136 been achieved from the Solecki lab (Kullmann et al., 2020).

137 ### Hippocampus dissection and neuron isolation

138 One day before neuron isolation, glass cover slips (13 mm diameter, VWR) were
139 placed into 24 well plates and coated overnight with 0.1 mg/ml poly-L-lysine
140 hydrobromid (dilution of 1 mg/ml poly-L-lysine with 0.1 M boric acid at pH 8.5) in a
141 humidified incubator at 37°C and 5% CO_2. For replating, 24 well plates without cover
142 slips were coated with 0.05 mg/ml poly-L-lysine hydrobromid and similar incubated
143 as above. On the day of neuron isolation, plates were washed twice with ddH_2O and
144 equilibrated either with 500 µl nucleofection medium (DMEM-31966 (Gibco)
145 supplemented with 10% FBS (Gibco) or for non-nucleofected neurons with
146 neurobasal (NB, Gibco) medium. Mice of either sex were sacrificed at embryonic day
147 18.5 (E18.5) by decapitation, and brains were dissected on ice in Leibovitz's L15-
148 Medium with 7 mM HEPES (L15+H, Gibco). After removal of the meninges,
149 hippocampi of each embryo were isolated and collected in a tube containing cooled
150 L15+H. Thereafter, medium was replaced by 500 µl pre-warmed TrypLE™ Express
151 (Gibco) per embryo and incubated for 6 min at 37°C. Subsequently, hippocampi
152 were washed twice with neurobasal medium containing 2% B27, 2 mM GlutaMax,
153 100 µg/ml streptomycin, and 100 U/ml penicillin (NB+, Gibco). After washing,
154 neurons were triturated in 1 ml NB+ by pipetting seven times up and down with a
155 P1000 pipette. Neuron solution was filled up to 1ml NB+ medium per embryo and

eNeuro Accepted Manuscript

156 density was calculated by using a hemocytometer. Thereafter, neurons were plated
157 at a density of 60,000 cells per well. 5 h after plating, medium was completely
158 replaced by NB+ medium.

159 **Electroporation of hippocampal neurons**

160 In some experiments, neurons were electroporated prior to plating. In these
161 experiments, electroporation was performed according to manufacturer's protocol by
162 using the Amaxa™ P3 Primary Cell 4D-Nucleofector™ X Kit L (Lonza) and 4D-
163 Nucleofector® (Lonza). For nucleofection, 250,000 neurons were transfected with 3
164 µg plasmid and the entire neuron suspension was plated in a single well of a 24 well
165 plate in nucleofection medium. 5 h after plating, medium was completely replaced by
166 NB+ medium.

167 **Replating of hippocampal neurons**

168 At DIV2, neurons were detached and plated again (replated) on cover slips. Before
169 replating, coverslips were prepared as described above. For replating, condition
170 medium (350 µl medium from each well + 200 µl fresh NB+ medium for each well)
171 was collected and kept in the water bath at 37°C. Remaining medium was aspirated,
172 replaced with pre-warmed 500 µl TrypLE™ Express per well and incubated for 15
173 min in the humidified incubator. To detach the cells after incubation, the bottom of
174 the well was rinsed twice with the TrypLE™ Express, and 500 µl pre-warmed NB+
175 medium was added to stop enzymatic reaction. Again the bottom of the well was
176 rinsed twice with the medium-enzyme solution and then completely transferred in to
177 1.5 ml cups and centrifuged for 5 min with 7,000 rpm. Thereafter, pelleted neurons
178 were re-suspended in 500 µl condition medium and plated on cover slips in 24 well
179 plates and incubated at 37°% with 5% CO_2 until further processing.

180 **Immunocytochemistry**

181 One or two days after seeding or replating, neurons were fixed for 10 min in 4%
182 paraformaldehyde in PBS under cytoskeleton preserving conditions (pH 7-7.5). After
183 washing with PBS, neurons were incubated with 0.4% gelatin with 0.5% Triton-X100
184 in PBS (carrier solution) for 5 min, followed by incubation with the primary antibody
185 rabbit anti-Dcx (1:500, Abcam; in carrier solution). After 90 min incubation, neurons
186 were washed with PBS and incubated with AlexaFluor488-coupled Phalloidin (1:100,
187 ThermoFisher Scientific) to visualize F-actin and the secondary antibody anti-rabbit

eNeuro Accepted Manuscript

188 IgG coupled to AlexaFluor546 (1:500, Invitrogen; in carrier solution). After 60 min of
189 incubation neurons were washed with PBS and nuclei were stained with the DNA
190 dye Hoechst (1:1,000 in PBS, Invitrogen). Neurons were imaged with a Leica TCS
191 SP5 II confocal microscope setup.

192 **Live cell imaging**

193 For live cell imaging, neurons were seeded either directly after nucleofection or after
194 replating in a poly-L-lysine hydrobromid coated 22 mm glass-bottom dish and
195 cultured for 1d. To measure actin turnover via fluorescence recovery after
196 photobleaching (FRAP), neurons were transfected with GFP-actin (Robert Grosse
197 lab) and imaged with a Leica TCS SP5 II in a chamber heated to 35°C. For imaging,
198 neurons were washed once and then imaged in CO_2-saturated HBS solution (Gibco),
199 supplemented with 4.16 mM $NaHCO_3$ and 2 mM $CaCl_2$. For pre-bleaching condition,
200 5 images of growth cones were acquired and in total 65 images over a time course
201 of 5 min during fluorescence recovery. Images were analyzed with ImageJ
202 (Schindelin et al., 2012) and recovery curve and parameters were calculated with R.
203 To assess retrograde F-actin flow of growth cones neurons were transfected with
204 LifeAct-GFP (Robert Grosse lab) and imaged in a CO_2-regulated chamber
205 maintained at 37°C. Image acquisition was done with a Leica DMi8 Thunder
206 microscope system and a Leica DFC9000 GTC camera, which acquired images
207 every 5 s for 5 min. Kymograph generation and analysis was performed with ImageJ
208 (Schindelin et al., 2012).

209 **Growth cone collapse assay and BDNF treatment**

210 Neurons were treated for 60 min with 100 ng/ml BDNF (PeproTech), 1 µg/µl Ephrin
211 A5 (R&D System) or 1 µg/µl Slit-1 (R&D System) before fixation. Images were
212 acquired with a Leica TCS SP5 II microscope system and analyses were done with
213 ImageJ (Schindelin et al., 2012). Growth cone size was measured for determining
214 BDNF effects, whereas repellent cues treated growth cones were categorized into
215 collapsed and non-collapsed according to previous studies (Müller et al.,
216 1990).**Statistics**

217 Statistical tests were done in R or Sigma Plot. For comparing mean values between
218 groups, student's t-test or Mann-Whitney U-test was performed. Analyzing the
219 rescue conditions, ANOVA with post-hoc test was used. Stage distribution and non-
220 collapsed vs. collapsed growth cones were tested for differences with $\chi 2$-test.

221

eNeuro Accepted Manuscript

222 ## Results

223 ### Replating does not alter hippocampal neuron morphology

224 This study aimed at testing whether a combination of nucleofection and replating is a
225 useful approach to study early aspects of hippocampal neuron differentiation. To do
226 so, we isolated hippocampal neurons from C57Bl/6 mice at embryonic day 18.5
227 (E18.5). Upon nucleofection, hippocampal neurons were seeded in 24 well plates
228 and incubated at standard conditions (Fig. 1). After two days in vitro (DIV2), we
229 detached neurons by means of an enzymatic digest and mechanical treatment to
230 reset them into an undifferentiated stage. Thereafter, hippocampal neurons were
231 plated on cover slips and kept in culture, similar to non-replated neurons. To test
232 whether this procedure affected neuron differentiation, we compared neurons one or
233 two days after replating (DAR) with non-replated neurons at DIV1 or DIV2,
234 respectively. We stained neurons with the F-actin marker phalloidin and an antibody
235 against doublecortin (Dcx) that labelled neurites (Fig. 2A). This approach allowed us
236 to categorize neurons according to their differentiation stage (Fig. 2B; Dotti et al.,
237 1988). As expected, only a few non-replated DIV1 neurons remained in stage 1, i.e.
238 they formed F-actin-enriched lamellipodia, but not yet neurites (Fig. 2C). The
239 majority developed neurites, but not yet an axon and were assigned to stage 2, while
240 a few neurons already possessed an axon and reached stage 3 ((in %) stage 1:
241 9.48±2.55; stage 2: 79.95±4.43, stage 3: 10.56±2.83, n>180 cells from 3
242 independent experiments). Very similar to non-replated DIV1 neurons, we found a
243 few neurons in stage 1 and stage 3 at DAR1, while the majority were assigned to
244 stage 2 ((in %) stage 1: 13.05±2.02; stage 2: 77.59±2.90, stage 3: 9.36±2.25,
245 n>340/3). Comparison between DIV1 and DAR1 cultures revealed no difference in
246 stage distribution (P=0.44). At DIV2, the fraction of non-replated stage 3 neurons
247 increased to roughly one third, and almost all other neurons were in stage 2 ((in %)
248 stage 1: 4.81±2.22, stage 2: 57.39±4.17, stage 3: 37.80±3.10; n>160/3). We found a
249 similar stage distribution among DAR2 neurons ((in %) stage 1: 5.32±1.59, stage 2:
250 56.97±3.71, stage 3: 37.71±4.56; n>240/3), with no difference when compared to
251 DIV2 cultures (P=0.81).

252 Antibody staining further allowed us to determine neuron morphology by counting the
253 numbers of primary neurites and neurite endpoints and by calculating the ratio of
254 primary neurites and neurite endpoints as a readout for neuron complexity. We

eNeuro Accepted Manuscript

255 determined these parameters in stage 2 neurons at DAR1 and DAR2 and compared
256 them to non-replated neurons at DIV1 and DIV2, respectively. In DAR1 neurons, the
257 numbers of primary neurites and neurite endpoints was not different from DIV1
258 neurons (Fig. 2D-E; neurites: DIV1: 5.11±0.38, DAR1: 4.83±0.25, P=0.54; endpoints:
259 DIV1: 5.50±0.39, DAR1: 5.90±0.33, P=0.44). Instead, the neurite/endpoint ratio was
260 slightly increased by roughly 10% in DAR1 neurons (Fig. 2F; DIV1: 1.10±0.05,
261 DAR1: 1.24±0.05, P<0.05; n>20/3). Compared to DIV2 neurons, the neurite and
262 endpoint numbers were slightly reduced by 8% and 30%, respectively, in DAR2
263 neurons (Fig. 2D-E; neurites: DIV2: 4.49±0.26, DAR2: 4.12±0.28, P<0.05; endpoints:
264 DIV2: 7.67±0.70, DAR2: 5.38±0.41, P<0.01; n>20/3). However, neuron complexity
265 was similar to DIV2 neurons in DAR2 neurons (Fig. 2F; DIV2: 1.55±0.11, DAR2:
266 1.33±0.09, P=0.12). Together, stage distribution did not differ between DAR1 and
267 DIV1 cultures or between DAR2 and DIV2 cultures. Likewise, gross morphology of
268 DAR1 and DAR2 neurons was similar to DIV1 and DIV2 neurons, respectively, and
269 DAR2 neurons showed only minor changes in morphology.

270

271 **Replating does not alter growth cone size or morphology**

272 Next, we tested whether replating altered the morphology or function of growth
273 cones, which are relevant for directed neurite outgrowth and neurite navigation
274 through the developing brain. First, we exploited phalloidin-labelled neurons to
275 determine growth cone size and morphology (Fig. 3A). For better comparison, we
276 restricted this analysis to stage 2 neurons. In DIV1 and DIV2 neurons, growth cones
277 size reached roughly 20 or 30 μm^2, respectively (Fig. 3B; (in μm^2) DIV1: 23.05±1.74,
278 n>70/3; DIV2: 30.86±2.25, n>70/3). Growth cone size did not differ from non-
279 replated DIV1 or DIV2 neurons in neurons from DAR1 or DAR2 cultures, respectively
280 ((in μm^2) DAR1: 20.33±1.00, n>100/3, P=0.18; DAR2: 29.97±1.95, n>100/3,
281 P=0.76). Growth cone morphology was assessed by determining growth cone
282 circularity (area divided by perimeter) and solidity (growth cone area divided by hull
283 area), similar to previous studies (Chitsaz et al., 2015; Dos-Santos et al., 2020). Both
284 parameters were not different between growth cones from DAR1 and DIV1 neurons
285 (Fig. 3C; solidity: DIV1: 0.63±0.02, n>70/3, DAR1: 0.60±0.01, n>90/3, P=0.20;
286 circularity: DIV1: 0.22±0.02, n>70/3, DAR1: 0.25±0.01, n>90/3, P=0.33). Together,
287 replating neither affected growth cone size nor morphology.

eNeuro Accepted Manuscript

288 **Replating does not alter actin dynamics in growth cones**

289 Next, as functional readouts, we assessed actin dynamics in replated neurons. We
290 electroporated neurons prior to seeding to express GFP-actin that allowed us to
291 determine actin turnover in growth cones by fluorescence recovery after
292 photobleaching (FRAP), similar to previous studies (Flynn et al., 2012). We
293 performed FRAP experiments in growth cones from DAR1 neurons and compared
294 actin turnover to growth cones from non-replated DIV1 neurons. In growth cones
295 from DIV1 neurons, GFP-actin rapidly recovered with a mean half-recovery time ($t_{½}$)
296 of 77.36±12.29 s (n>20/3; Fig. 4A-C; Movie 1). We noted a similar GFP-actin
297 recovery in growth cones from DAR1 neurons, with no difference in $t_{½}$ (Fig. 4A-C;
298 Movie 2; (in s) 74.04±10.00, n>20/3, P=0.83). Further, we calculated the stable actin
299 fraction that did not recover within the time frame of 300 s. This fraction was not
300 different between growth cones from DIV1 and DAR1 neurons (Fig. 4D; DIV1:
301 0.78±0.03, DAR1: 0.75±0.03, P=0.500). Additionally, we electroporated neurons
302 before plating to express LifeAct-GFP, which allowed us to visualize F-actin in living
303 neurons (Flynn et al., 2012; Riedl et al., 2008). F-actin appeared similarly dynamic in
304 growth cones from DAR1 and DIV1 neurons (Movies 3-4). Indeed, kymograph
305 analysis revealed similar average retrograde flow velocity of F-actin in growth cones
306 from both groups (Fig. 4E-F; (in µm/min) DIV1: 8.18±1.58, n>20/3, DAR1: 7.73±0.82,
307 n>50/3, P=0.80). Together, replating neither affected actin turnover nor retrograde F-
308 actin flow in growth cones.

309

310 **Growth cones from replated neurons respond normally to guidance cues**

311 Apart from studying actin dynamics, we tested whether growth cones from neurons
312 of both groups respond differently to guidance cues. First, we determined growth
313 cone size in phalloidin-stained DIV1 and DAR1 neurons upon treatment with the
314 neurotrophin brain-derived neurotrophic factor (BDNF). As expected (Meier et al.,
315 2011), BDNF increased growth cone size in non-replated neurons by 62% when
316 compared to PBS-treated controls (Fig. 5A-B; (in $µm^2$) PBS: 29.17±1.35, BDNF:
317 47.13±2.40, P<0.001, n>130/3). BDNF similarly increased growth cone size in DAR1
318 neurons (in $µm^2$) PBS: 31.30±1.59, BDNF: 56.45±3.48, P<0.001, n>100/3). Hence,
319 growth cones from DIV1 and DAR1 neurons respond similarly to BDNF.

eNeuro Accepted Manuscript

320 Second, we investigated the effects of two different repellent cues, namely Ephrin A5
321 (EphA5) and Slit-1, on growth cones from non-replated and replated neurons (Meier
322 et al., 2011; Ye et al., 2019). As a readout, we determined the fraction of collapsed
323 growth cones in phalloidin-stained neurons upon treatment with either EphA5 or Slit-
324 1 and compared these fractions to PBS-treated control neurons (Fig. 5C). In
325 agreement with normal growth cone morphology in replated neurons, the fraction of
326 collapsed growth cones did not differ between DIV1 and DAR1 neurons before
327 guidance cue treatment (Fig. 5D; (in %) DIV1: 20.71±2.15, DAR1: 20.20±2.19,
328 P=0.89, n>200/3). EphA5 and Slit-1 increased the fraction of collapsed growth cones
329 roughly threefold in DIV1 neurons (EphA5: 60.95±2.59, P<0.001, n>300/3; Slit-1:
330 53.67±3.17, P<0.001, n>300/3). Similarly, both repellent cues strongly increased the
331 fraction of collapsed growth cones in DAR1 neurons (EphA5: 58.80±6.26, P<0.001,
332 n>210/3; Slit-1: 50.80±4.04, P<0.001, n>200/3). Together, growth cones from non-
333 replated and replated neurons respond similarly to the neurotrophin BDNF as well as
334 the repellent cues EphA5 and Slit-1.

335

336 **Nucleofection-mediated gene inactivation allows to study early aspects of**
337 **neuron differentiation in replated neurons**

338 The aforementioned approaches to test growth cone actin dynamics in replated
339 neurons were based on nucleofection-based reporter gene expression. To extend
340 our characterization of replated neurons to gene inactivation, we exploited primary
341 hippocampal neurons from gene targeted mice ($ADF^{-/-}/Cfl1^{flx/flx}$) lacking the actin-
342 binding protein ADF and additionally carrying a floxed allele of the ADF homolog
343 cofilin1 (Bellenchi et al., 2007). We chose this mouse model for a proof of concept,
344 because actin-depolymerizing proteins of the ADF/cofilin family have been previously
345 implicated in growth cone morphology (Gomez et al., 2014; Omotade et al., 2017),
346 and because previous studies revealed redundant functions of ADF and cofilin1 in
347 neurons (Zimmermann et al., 2015; Wolf et al., 2015; Flynn et al., 2012). To
348 inactivate cofilin1, we electroporated $ADF^{-/-}/Cfl1^{flx/flx}$ neurons prior to initial seeding
349 with mCherry-tagged Cre recombinase (Cre), $ADF^{-/-}/Cfl1^{flx/flx}$ neurons expressing a
350 catalytically inactive mCherry-Cre variant (Cre-mut) served as controls (Kullmann et
351 al., 2020). We fixed Cre- and Cre-mut-expressing $ADF^{-/-}/Cfl1^{flx/flx}$ neurons at either
352 DIV1 or DAR1 and determined growth cone size upon phalloidin staining (Fig. 6A).

eNeuro Accepted Manuscript

353 At DIV1, we found that growth cone size in Cre-expressing ADF$^{-/-}$/Cfl1$^{flx/flx}$ neurons
354 was not different from Cre-mut-expressing controls (Fig. 6B; (in μm^2) Cre-mut:
355 26.5±1.72, Cre: 25.96±1.95, P=0.100, n>30/3). Instead, growth cone size was
356 strongly increased in Cre-expressing ADF$^{-/-}$/Cfl1$^{flx/flx}$ neurons at DAR1 when
357 compared to Cre-mut-expressing controls ((in μm^2) Cre-mut: 24.40±2.2, Cre:
358 48.50±3.74, P<0.001, n>80/3). Hence, ADF$^{-/-}$/Cfl1$^{flx/flx}$ neurons displayed the
359 expected increase in growth cone size upon genetic inactivation of ADF and cofilin1
360 at DAR1, but not at DIV1. Together, our replating protocol together with
361 nucleofection-based gene inactivation prior to initial seeding allowed us to study the
362 relevance of a gene of interest for early processes of neuron differentiation, thereby
363 highlighting the utility of our approach.

eNeuro Accepted Manuscript

364 ## Discussion

365 In the present study we report a protocol to reset DIV2 primary mouse hippocampus
366 neurons into an undifferentiated stage. We combined replating with nucleofection-
367 based genetic manipulation (both reporter gene expression as well as gene
368 inactivation by exploiting the Cre/loxP system) prior to initial seeding of primary
369 neurons. This approach allows a thorough analysis of neuron differentiation including
370 early processes such as neurite formation and outgrowth or growth cone function.

371 Replating of cultured neurons has been reported for various neuron subtypes
372 including primary dorsal root ganglia (DRG) neurons, primary cortical neurons or
373 stem cell (SC)-derived neurons (Biswas et al., 2018; Calabrese et al., 2019;
374 Caviedes et al., 1990a; Caviedes et al., 1990b; Frey et al., 2015; Koechling et al.,
375 2011; Saijilafu et al., 2013; Lee et al., 2020). Neuron replating has been
376 implemented to reduce neuron complexity and cell membrane surface area, thereby
377 improving accessibility for electrophysiological recordings, because passive
378 membrane properties such as membrane capacitance or resistance were altered
379 (Caviedes et al., 1990a; Caviedes et al., 1990b). Further, it has been implemented to
380 transfer SC-derived neurons from normal cell culture dishes onto 384 wells prior to
381 experiments (Calabrese et al., 2019), and it has been exploited as a paradigm of
382 axon regeneration (Frey et al., 2015; Saijilafu et al., 2013; Lee et al., 2020). These
383 studies differed in the procedure applied, and some of them only included a brief and
384 rather superficial description of the method. Moreover, these studies either did not
385 focus on early aspects of neuron differentiation, did not systematically compare non-
386 replated and replated neurons or did not combine replating with genetic
387 manipulation. Hence, it remained unknown whether differentiation of replated
388 neurons differed from non-replated neurons and whether a combination of genetic
389 manipulation prior to initial seeding and replating allowed to study early aspects of
390 neuron differentiation.

391 We compared cultured mouse hippocampal neurons that have been replated at DIV2
392 with non-replated neurons, focusing on early aspects of neuron differentiation up to
393 two days after replating. Our comparison included a categorization of neurons
394 according to their differentiation stage as well as a thorough morphometric analysis.
395 Neuron categorization did not reveal any differences between non-replated and
396 replated neurons, thereby demonstrating that differentiation was largely preserved in

eNeuro Accepted Manuscript

397 replated neurons. Likewise, gross morphology was normal in replated neurons.
398 However, they displayed some changes in neuron morphology, which are likely not
399 biologically relevant. Our data demonstrated that our replating procedure
400 successfully reset DIV2 primary hippocampal neurons into an undifferentiated stage
401 and that replated neurons differentiated very similar to non-replated neurons. Hence,
402 replated neurons faithfully reflect normal differentiation of hippocampal neurons.

403 Further, we combined our replating procedure with nucleofection-based transfection
404 of hippocampal neurons prior to initial seeding. We expressed reporter genes such
405 as GFP-actin or LifeAct-GFP that allowed us to determine actin turnover as well as
406 F-actin dynamics in growth cones as functional readouts. By FRAP analysis, we
407 found that actin turnover in growth cones was not different between replated and
408 non-replated neurons. Similarly, retrograde F-actin flow was unchanged in replated
409 neurons. These finding demonstrated that our replating procedure did not alter actin
410 dynamics in growth cones and let us suggest normal growth cone functions in
411 replated neurons. Indeed, growth cones from replated neurons did not differ to those
412 from non-replated neurons in their response to the neurotrophin BDNF or the
413 repellent cues EphA5 and Slit-1. Together, our analysis in hippocampal neurons did
414 not reveal any gross defects in differentiation, morphology or growth cone function in
415 hippocampal neurons induced by the replating procedure. In contrast to our findings,
416 a recent study revealed functional differences between non-replated and replated
417 DRG neurons. Specifically, this study showed that axon regeneration occurred in
418 replated adult DRG neurons even when gene transcription was inhibited by blocking
419 RNA polymerase II, while axon formation and outgrowth in non-replated adult DRG
420 neurons required RNA polymerase II activity (Saijilafu et al., 2013). However, it
421 remained unknown whether such functional differences between replated and non-
422 replated neurons is restricted to a specific cell types, i.e. adult DRG neurons, or
423 whether these differences are present in all CNS and PNS neurons.

424 Apart from nucleofection of reporter genes, we exploited the Cre/loxP system to
425 genetically remove actin-depolymerizing proteins of the ADF/cofilin family that have
426 been previously linked to growth cone morphology (Gomez et al., 2014; Omotade et
427 al., 2017). While growth cone size was unchanged in non-replated Cre-expressing
428 ADF$^{-/-}$/Cfl1$^{flx/flx}$ neurons at DIV1, it was strongly increased in replated Cre-expressing
429 ADF$^{-/-}$/Cfl1$^{flx/flx}$ neurons at DAR1. Differences in growth cone size between Cre-

430 expressing $ADF^{-/-}/Cfl1^{flx/flx}$ neurons at DIV1 and DAR1 can be easily explained by the
431 fact that DAR1 neurons were two days longer in culture when compared to DIV1
432 neurons. Thus, DAR1 neurons had longer time to express Cre and to recombine the
433 genome and, hence, to genetically remove cofilin1. In line with this, previous studies
434 showed residual cofilin1 levels up to a few days upon beginning of Cre expression in
435 the mouse brain, but also in various cell types including isolated hippocampal
436 neurons (Bellenchi et al., 2007; Rust et al., 2010; Flynn et al., 2012; Rehklau et al.,
437 2012). Together, these data demonstrated that our replating protocol in combination
438 with nucleofection-based gene inactivation allows us to study the relevance of a
439 gene of interest for early aspects of neuron differentiation, different from
440 nucleofected non-replated neurons. Hence, nucleofection combined with our
441 replating protocol enables a more thorough analysis of neuron differentiation when
442 compared to neurons that were nucleofected, but not replated.

443 In summary, we report a protocol to reset DIV2 primary mouse hippocampal neurons
444 into an undifferentiated stage. This procedure is compatible with nucleofection-based
445 genetic manipulation of primary neurons prior to their initial seeding. Our approach
446 allowed us i) to express fluorescent reporters during neuron differentiation that are
447 needed to address specific biological processes such as actin dynamics in growth
448 cones or ii) to inactivate a gene of interest in order to study its function in early
449 aspects of neuron differentiation. This approach is highly flexible, straightforward and
450 far less labor-intensive and expensive than previous approaches, i) in which
451 transgenic mice such as Lifeact-expressing strains were exploited to study actin
452 dynamics during early differentiation in cultured hippocampal neurons (Flynn et al.,
453 2012) or ii) which required the breeding and scarification of a large number of
454 knockout mice and their control littermates. Hence, our replating protocol is very
455 helpful to reduce the number of experimental animals, and it thereby complies with
456 the 3R principle for a more ethical use of animals in biomedical research (Russell et
457 al., 1959; Lee et al., 2020). While we here used expression of fluorescent reporters
458 and Cre/loxP-based gene inactivation for a proof of principle, genetic manipulation
459 can be easily expanded to gene silencing via RNA interference or other modes of
460 gene deletion, e.g. by exploiting the CRISPR/Cas system. Taken together, a
461 combination of nucleofection and replating of primary mouse hippocampal neurons is

eNeuro Accepted Manuscript

eNeuro Accepted Manuscript

462 a powerful and versatile approach to comprehensively study the molecular
463 mechanisms regulating neuron differentiation.

464

465 ## References

466 Bellenchi GC, Gurniak CB, Perlas E, Middei S, Ammassari-Teule M, Witke W (2007)
467 N-cofilin is associated with neuronal migration disorders and cell cycle control in
468 the cerebral cortex. Genes Dev 21:2347-57.

469 Biswas S, Kalil K (2018) The Microtubule-Associated Protein Tau Mediates the
470 Organization of Microtubules and Their Dynamic Exploration of Actin-Rich
471 Lamellipodia and Filopodia of Cortical Growth Cones. J Neurosci 38:291-307.

472 Calabrese B, Powers RM, Slepian AJ, Halpain S (2019) Post-differentiation
473 Replating of Human Pluripotent Stem Cell-derived Neurons for High-content
474 Screening of Neuritogenesis and Synapse Maturation. J Vis Exp 2019 Aug
475 28;(150)

476 Caviedes P, Ault B, Rapoport SI (1990a) Replating improves whole cell voltage
477 clamp recording of human fetal dorsal root ganglion neurons. J Neurosci Methods
478 35:57-61.

479 Caviedes P, Ault B, Rapoport SI (1990b) The role of altered sodium currents in
480 action potential abnormalities of cultured dorsal root ganglion neurons from
481 trisomy 21 (Down syndrome) human fetuses. Brain Res 510:229-36.

482 Chitsaz D, Morales D, Law C, Kania A (2015) An Automated Strategy for Unbiased
483 Morphometric Analyses and Classifications of Growth Cones In Vitro. PLoS One
484 10:e0140959.

485 da Silva JS, Dotti CG (2002) Breaking the neuronal sphere: regulation of the actin
486 cytoskeleton in neuritogenesis. Nat Rev Neurosci 3:694-704.

487 Dos-Santos Carvalho S, Moreau MM, Hien YE, Garcia M, Aubailly N, Henderson DJ,
488 Studer V, Sans N, Thoumine O, Montcouquiol M (2020) Vangl2 acts at the
489 interface between actin and N-cadherin to modulate mammalian neuronal
490 outgrowth. Elife 9:e51822.

491 Dotti CG, Sullivan CA, Banker GA (1988) The establishment of polarity by
492 hippocampal neurons in culture. J Neurosci 8:1454-68.

493 Dudek H, Ghosh A, Greenberg ME (2001) Calcium phosphate transfection of DNA
494 into neurons in primary culture. Curr Protoc Neurosci Chapter 3: Unit 3 11.

eNeuro Accepted Manuscript

eNeuro Accepted Manuscript

495 Flynn KC, Hellal F, Neukirchen D, Jacob S, Tahirovic S, Dupraz S, Stern S, Garvalov
496 BK, Gurniak C, Shaw AE, Meyn L, Wedlich-Soldner R, Bamburg JR, Small JV,
497 Witke W, Bradke F (2012) ADF/Cofilin-Mediated Actin Retrograde Flow Directs
498 Neurite Formation in the Developing Brain. Neuron 76:1091-107.

499 Frey E, Valakh V, Karney-Grobe S, Shi Y, Milbrandt J, DiAntonio A (2015) An in vitro
500 assay to study induction of the regenerative state in sensory neurons. Exp Neurol
501 263: 350-63.

502 Gomez TM, Letourneau PC (2014) Actin dynamics in growth cone motility and
503 navigation. J Neurochem 129:221-34.

504 Koechling T, Khalique H, Sundstrom E, Avila J, Lim F (2011) A culture model for
505 neurite regeneration of human spinal cord neurons. J Neurosci Methods 201:346-
506 54.

507 Kullmann JA, Trivedi N, Howell D, Laumonnerie C, Nguyen V, Banerjee SS, Stabley
508 DR, Shirinifard A, Rowitch DH, Solecki DJ (2020) Oxygen tension and the VHL-
509 Hif1alpha pathway determine onset of neuronal polarization and cerebellar
510 germinal zone exit. Neuron 106:607-623.

511 Lee KH, Lee DW, Kang BC (2020) The 'R' principles in laboratory animal
512 experiments. Lab Anim Res 36:45.

513 Lee J, Shin JE, Lee B, Kim H, Jeon Y, Ahn SH, Chi SW, Cho Y (2020) The stem cell
514 marker Prom1 promotes axon regeneration by down-regulating cholesterol
515 synthesis via Smad signaling. Proc Natl Acad Sci USA 117:15955-15966.

516 Meier C, Anastasiadou S, Knöll B (2011) Ephrin-A5 suppresses neurotrophin evoked
517 neuronal motility, ERK activation and gene expression. PLoS One 6:e26089.

518 Müller B, Stahl B, and Bonhoeffer F (1990) In vitro experiments on axonal guidance
519 and growth-cone collapse. J Exp Biol 153:29-46.

520 Ohki EC, Tilkins ML, Ciccarone VC, Price PJ (2001) Improving the transfection
521 efficiency of post-mitotic neurons. J Neurosci Methods 112:95-9.

522 Omotade OF, Pollitt SL, Zheng JQ (2017). Actin-based growth cone motility and
523 guidance. Mol Cell Neurosci 84:4-10.

eNeuro Accepted Manuscript

524 Rehklau K, Gurniak CB, Conrad M, Friauf E, Ott M, Rust MB (2012) ADF/cofilin
525 proteins translocate to mitochondria during apoptosis but are not generally
526 required for cell death signaling. Cell Death Differ 19:958-967. Riedl J, Crevenna
527 AH, Kessenbrock K, Yu JH, Neukirchen D, Bista M, Bradke F, Jenne D, Holak TA,
528 Werb Z, Sixt M, Wedlich-Soldner R (2008) Lifeact: a versatile marker to visualize
529 F-actin. Nat Methods 5:605-607.

530 Russell WMS, Burch RL (1959) The principles of humane experimental technique.
531 London: Methuen and Co.

532 Rust MB, Gurniak CB, Renner M, Vara H, Morando L, Gorlich A, Sassoe-Pognetto
533 M, Banchaabouchi MA, Giustetto M, Triller A, Choquet D, Witke W (2010)
534 Learning, AMPA receptor mobility and synaptic plasticity depend on n-cofilin-
535 mediated actin dynamics. EMBO J 29:1889-1902.

536 Saijilafu, Hur EM, Liu CM, Jiao Z, Xu WL, Zhou FQ (2013) PI3K–GSK3 signalling
537 regulates mammalian axon regeneration by inducing the expression of Smad1.
538 Nat Commun 4:2690.

539 Schindelin J, Arganda-Carreras I, Frise E, Kaynig V, Longair M, Pietzsch T,
540 Preibisch S, Rueden C, Saalfeld S, Schmid B, Tinevez JY, White DJ, Hartenstein
541 V, Eliceiri K, Tomancak P, Cardona A (2012) Fiji: an open-source platform for
542 biological-image analysis. Nat Methods. 9:676-682.

543 Sun M, Bernard LP, Dibona VL, Wu Q, Zhang H (2013) Calcium phosphate
544 transfection of primary hippocampal neurons. J Vis Exp 81:e50808.

545 Viesselmann C, Ballweg J, Lumbard D, Dent EW (2011) Nucleofection and primary
546 culture of embryonic mouse hippocampal and cortical neurons. J Vis Exp 47:2373.

547 Wolf M, Zimmermann AM, Görlich A, Gurniak CB, Sassoè-Pognetto M, Friauf E,
548 Witke W, Rust MB (2015) ADF/Cofilin Controls Synaptic Actin Dynamics and
549 Regulates Synaptic Vesicle Mobilization and Exocytosis. Cereb Cortex 25:2863-
550 75.

551 Ye X, Qiu Y, Gao Y, Wan D, Zhu H (2019) A Subtle Network Mediating Axon
552 Guidance: Intrinsic Dynamic Structure of Growth Cone, Attractive and Repulsive
553 Molecular Cues, and the Intermediate Role of Signaling Pathways. Neural
554 Plasticity 2019:1719829.

555 Zeitelhofer M, Vessey JP, Thomas S, Kiebler M, Dahm R (2009) Transfection of
556 cultured primary neurons via nucleofection. Curr Protoc Neurosci Chapter 4: Unit
557 4.32.

558 Zimmermann AM, Jene T, Wolf M, Görlich A, Gurniak CB, Sassoè-Pognetto M,
559 Witke W, Friauf E, Rust MB (2015) Attention-Deficit/Hyperactivity Disorder-like
560 Phenotype in a Mouse Model with Impaired Actin Dynamics. Biol Psychiatry
561 78:95-106.

562

eNeuro Accepted Manuscript

eNeuro Accepted Manuscript

Figure Legends

Figure 1. Scheme showing experimental procedure. Timeline and workflow of experimental approach including i) isolation of hippocampal neurons from E18.5 mice, ii) electroporation-based genetic manipulation prior to seeding that could be either reporter gene expression or gene inactivation, iii) culture of hippocampal neurons for two days, iv) replating of hippocampal neurons at DIV2 to reset them into an undifferentiated stage, v) culture of replated neurons until further analyses. DIV: days *in vitro*, DAR: days after replating.

Figure 2. Replating neither alters differentiation nor gross morphology of hippocampal neurons. (A) Representative micrographs of mouse non-replated hippocampal neurons at DIV1 and DIV2 as well as DAR1 and DAR2. Neurons were stained with the F-actin marker phalloidin (green), with an antibody against doublecortin (Dcx, magenta) and the intercalating dye Hoechst (blue). **(B)** Representative micrographs of non-replated and replated stage 1, stage 2 and stage 3 neurons that have been used for morphometric analyses. **(C)** Stage distribution of non-replated and replated neurons. Graphs showing **(D)** numbers of primary neurites, **(E)** numbers of neurite endpoints as well as **(F)** primary neurite/neurite endpoint ratio in non-replated and replated neurons. Scale bars (in µm): 50 (A), 10 (B); ns: $P>0.05$, *: $P<0.05$, **: $P<0.01$. Green dots indicate mean values with standard error of the means.

Figure 3. Replating does not alter growth cone size or morphology in hippocampal neurons. (A) Representative micrographs of phalloidin-labelled growth cones from non-replated and replated stage 2 neurons. **(B)** Growth cone size of non-replated and replated stage 2 neurons. **(C)** Growth cone morphology (solidity, circularity) of non-replated and replated stage 2 neurons. Scale bar (in µm): 2 (A); ns: $P>0.05$. Green dots indicate mean values with standard error of the means.

Figure 4. Replating does not impair actin dynamics in growth cones. (A) Image sequence of growth cones from GFP-actin-expressing non-replated and replated

594 stage 2 neurons during FRAP analysis. **(B)** Recovery curves for GFP-actin in growth
595 cones from stage 2 neurons at DIV1 and DAR1. **(C)** Half-recovery time of GFP-actin
596 in growth cones during FRAP experiment. **(D)** Stable actin fraction in growth cones
597 during FRAP experiments. **(E)** Representative micrographs of growth cones from
598 LifeAct-GFP-expressing non-replated and replated neurons. Lines indicate where
599 kymographs (shown on the right) have been generated from. Arrows indicate the
600 retrograde F-actin flow. **(F)** Velocity of retrograde F-actin flow in growth cones. Scale
601 bars (in μm): 2 (A, D); ns: P>0.05. Green dots indicate mean values with standard
602 error of the means.

603

604 **Figure 5. Normal response to guidance cues in growth cones from replated**
605 **neurons. (A)** Representative micrographs of phalloidin-stained growth cones from
606 non-replated and replated neurons treated with either PBS or BDNF. **(B)** Growth
607 cone size in non-replated and replated neurons treated with either PBS or BDNF. **(C)**
608 Representative micrographs of phalloidin-stained collapsed and non-collapsed
609 growth cones from non-replated and replated neurons. **(D)** Fractions of collapsed
610 and non-collapsed growth cones in non-replated and replated neurons before and
611 after treatment with EphA5 and Slit-1. Scale bars (in μm): 2 (A, C); ns: P>0.05, ***:
612 P<0.001. Green dots in A indicate mean values with standard error of the means.

613

614 **Figure 6. Replating does not impair growth cone function in hippocampal**
615 **neurons. (A)** Representative micrographs of phalloidin-stained growth cones from
616 non-replated and replated $ADF^{-/-}/Cfl1^{flx/flx}$ neurons expressing either Cre or Cre-mut.
617 **(B)** Growth cone size in non-replated and replated $ADF^{-/-}/Cfl1^{flx/flx}$ neurons
618 expressing either Cre or Cre-mut. Scale bar (in μm): 2 (A); ns: P>0.05, ***: P<0.001.
619 Green dots indicate mean values with standard error of the means

620

621 **Movie 1:** Movie showing GFP-actin recovery upon bleaching in the growth cone of a
622 non-replated neuron at DIV1. Upon bleaching fluorescence recovery was recorded
623 over a time course of 3 min. Scale bar: 2 μm.

624

eNeuro Accepted Manuscript

eNeuro Accepted Manuscript

625 **Movie 2:** Movie showing GFP-actin recovery upon bleaching in the growth cone of a
626 replated neuron at DAR1. Upon bleaching fluorescence recovery was recorded over
627 a time course of 3 min. Scale bar: 2 µm.
628
629 **Movie 3:** Movie showing a growth cone from a LifeAct-GFP-transfected non-replated
630 neuron at DIV1. Images were acquired every 5 s for 5 min. Scale bar: 2 µm.
631
632 **Movie 4:** Movie showing a growth cone from a LifeAct-GFP-transfected replated
633 neuron at DAR1. Images were acquired every 5 s for 5 min. Scale bar: 2 µm.

eNeuro Accepted Manuscript

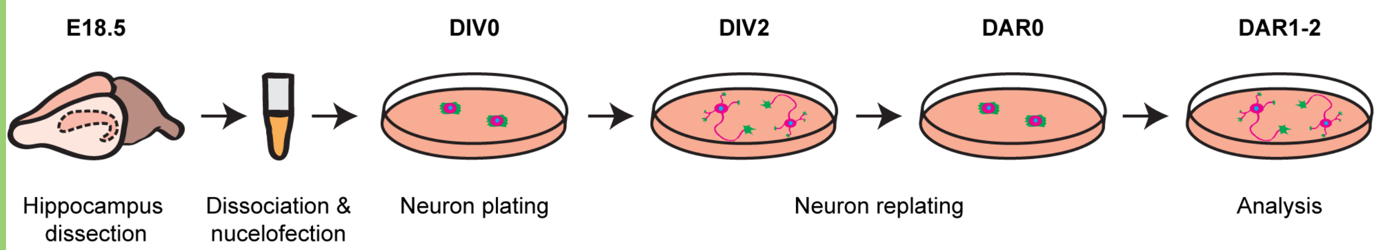

eNeuro Accepted Manuscript

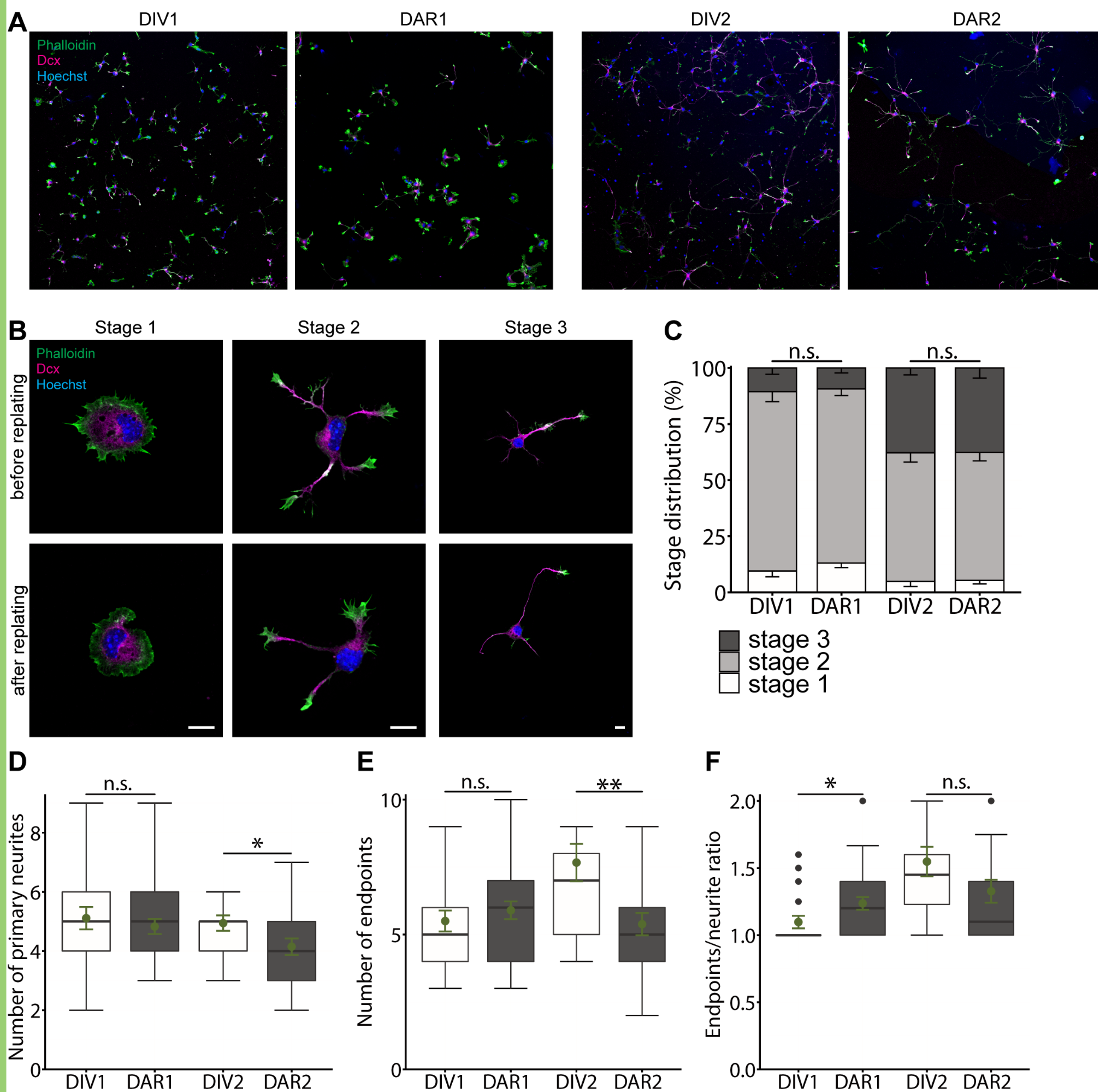

eNeuro Accepted Manuscript

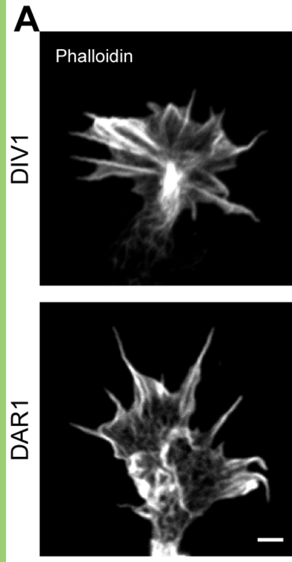

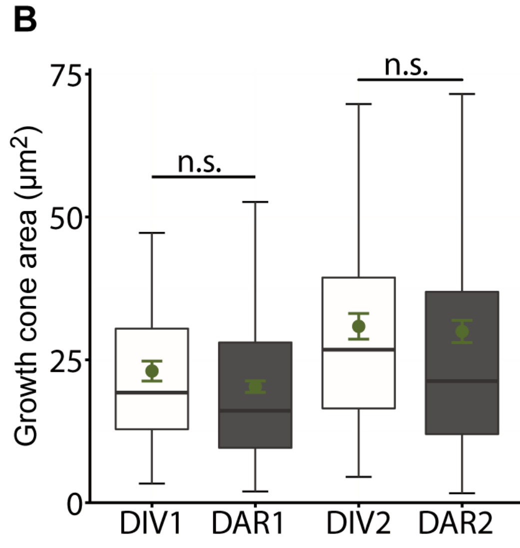

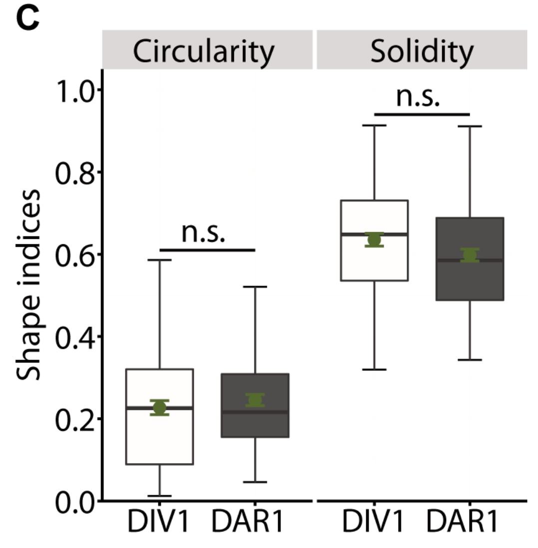

eNeuro Accepted Manuscript

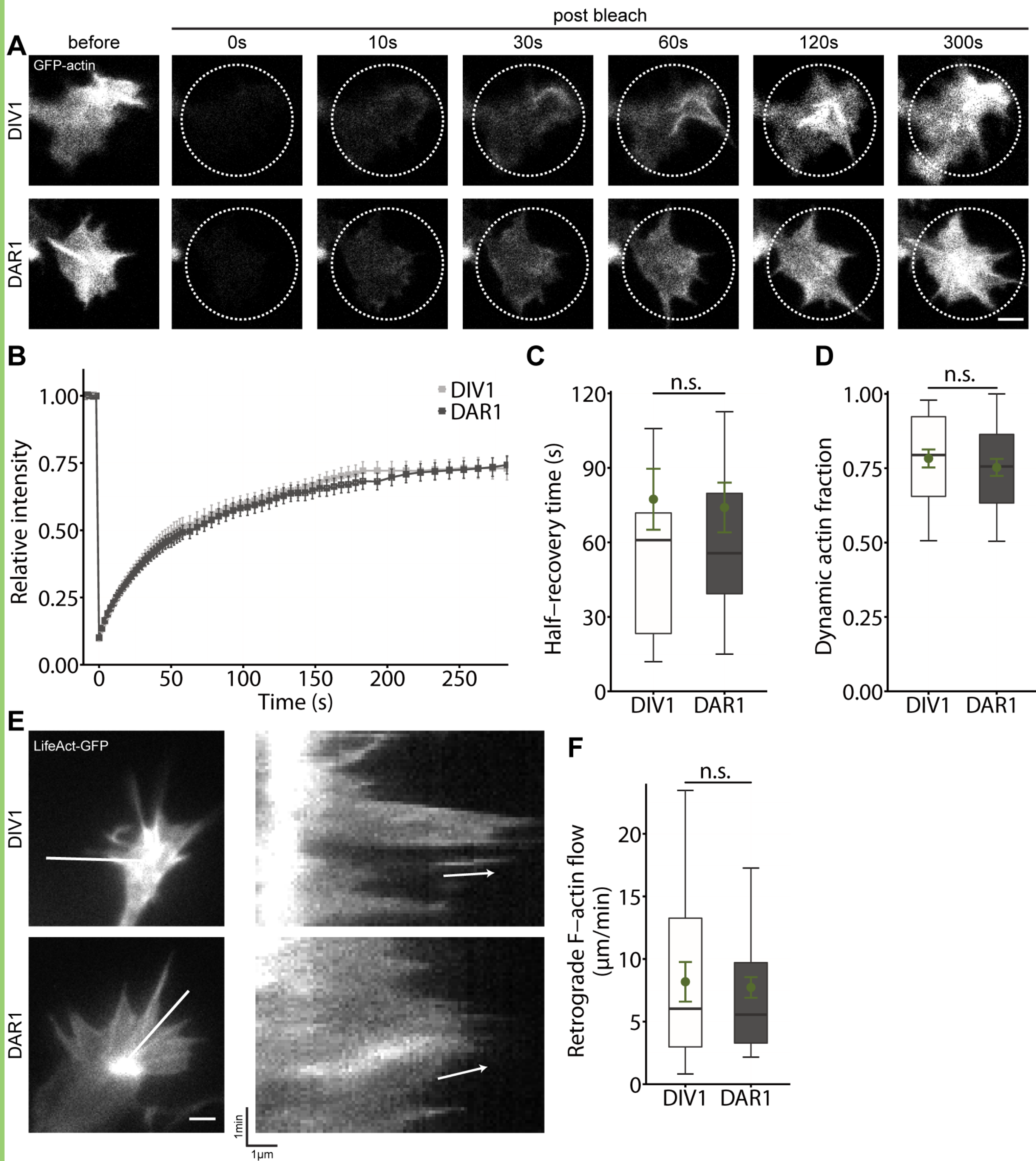

eNeuro Accepted Manuscript

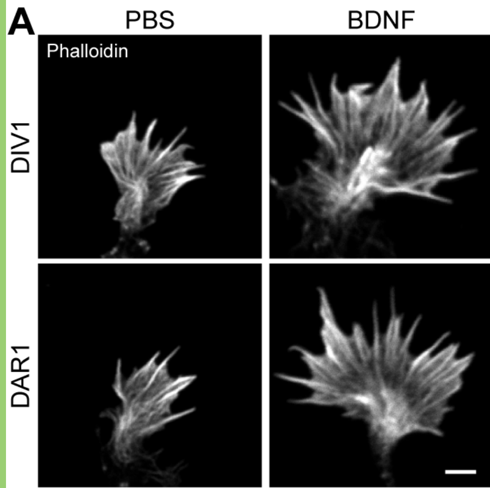

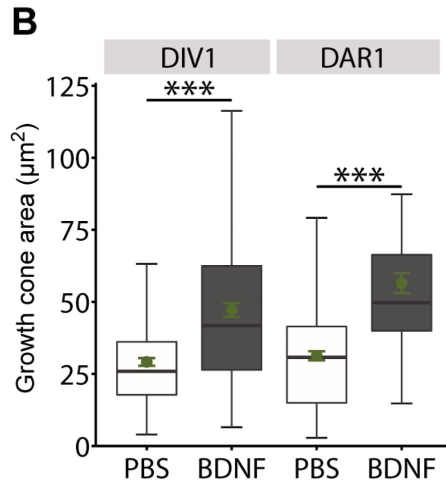

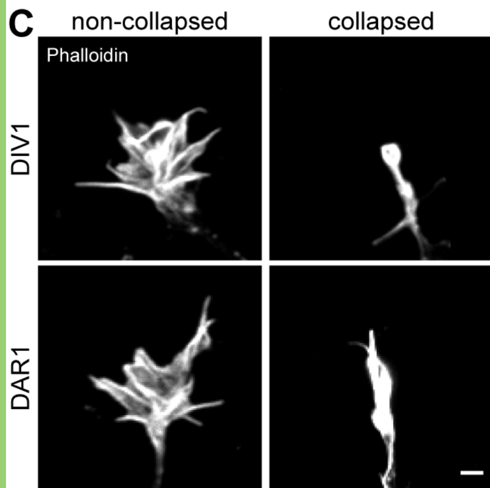

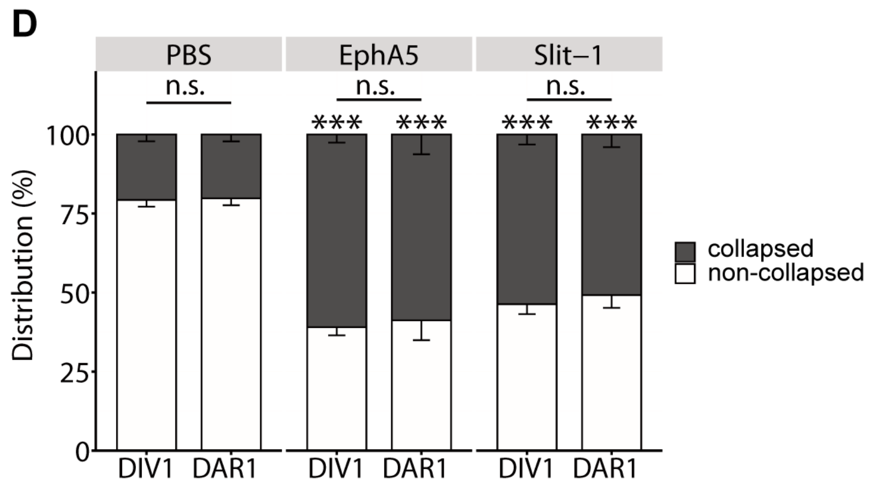

eNeuro Accepted Manuscript

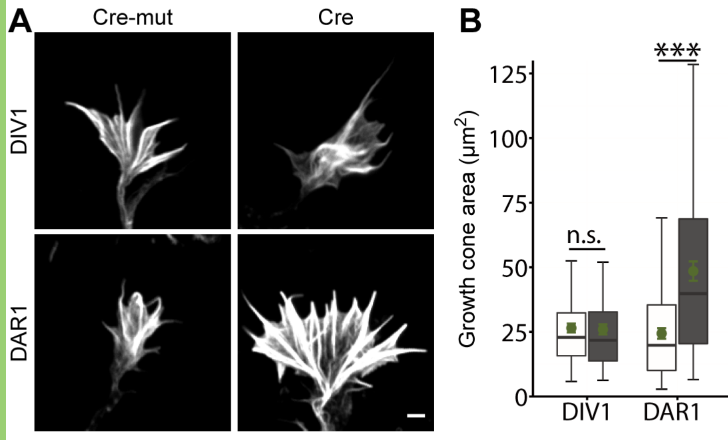

eNeuro Accepted Manuscript

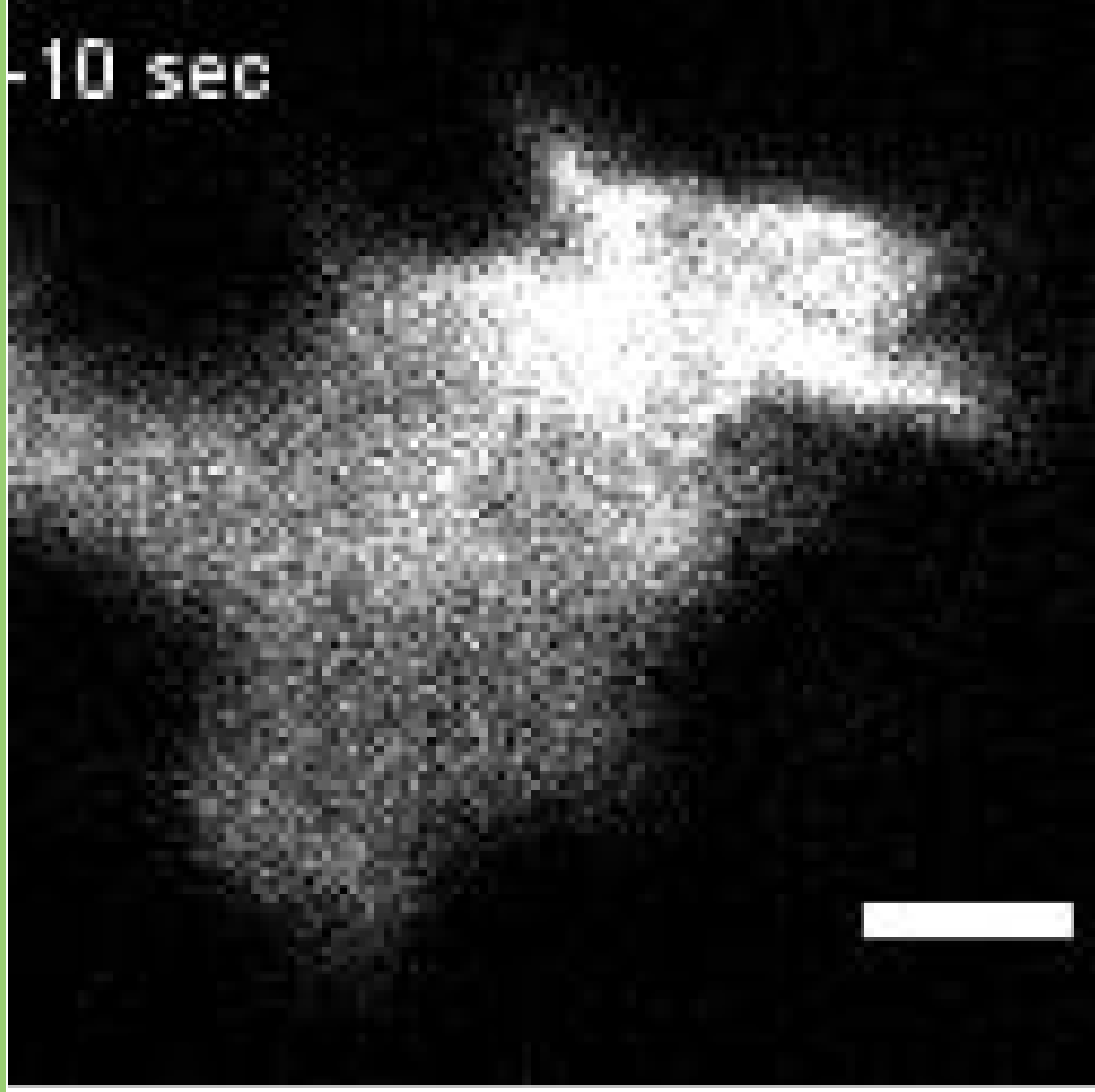

eNeuro Accepted Manuscript

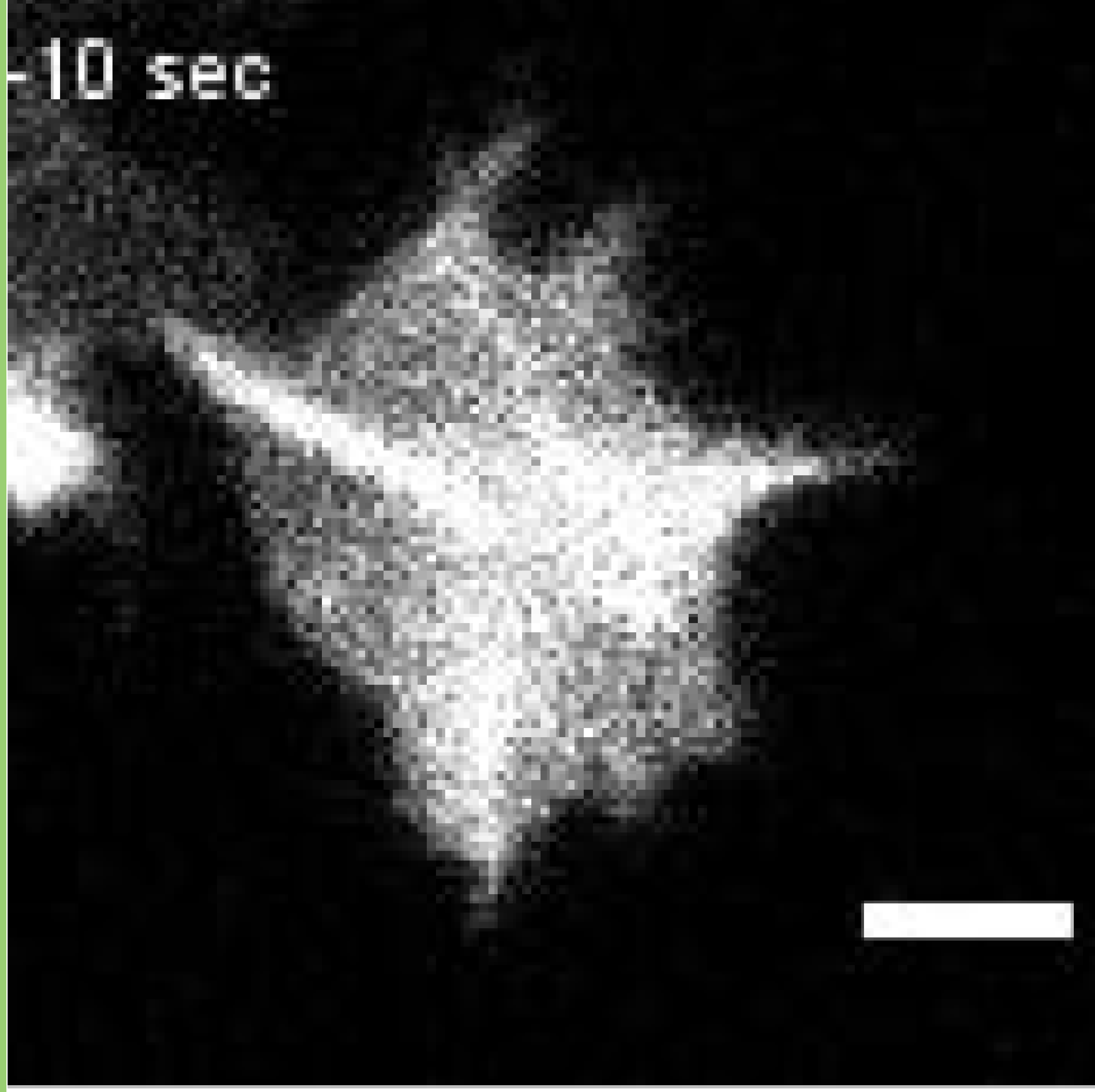

eNeuro Accepted Manuscript

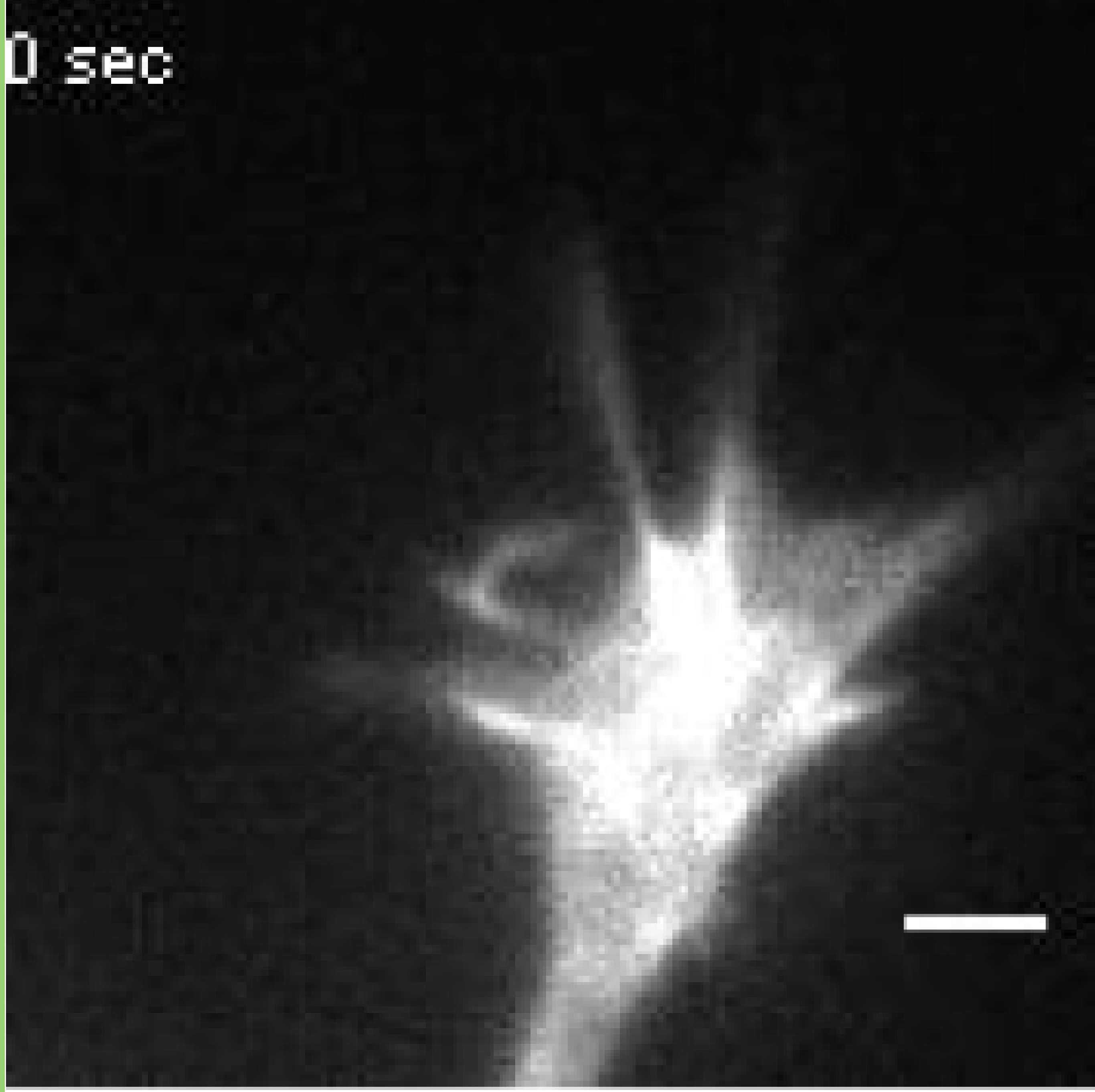

eNeuro Accepted Manuscript